Large-scale 3D printing of ultra-high performance concrete – a new processing route for architects and builders

Clément Gosselin, Romain Duballet, Philippe Roux, Nadja Gaudillière, Justin Dirrenberger, Philippe Morel

Large-scale 3D printing of ultra-high performance concrete – a new processing route for architects and builders

C. Gosselin [a,b], R. Duballet [a,b], Ph. Roux [a,b], N. Gaudillière [a,b], J. Dirrenberger [a,c,*], Ph. Morel [a,d,b]

[a] XtreeE SAS, 157 boulevard MacDonald, 75019 Paris, France
[b] Digital Knowledge, Ecole Nationale Supérieure d'Architecture Paris-Malaquais, 14 rue Bonaparte, 75006 Paris, France
[c] PIMM, Arts et Métiers-ParisTech/CNAM/CNRS UMR 8006, 151 bd de l'Hôpital, 75013 Paris, France
[d] EZCT Architecture & Design Research, 157 boulevard MacDonald, 75019 Paris, France

Keywords:
3D Printing
Concrete
Cementitious materials
Large-scale additive manufacturing
Architecture design

A B S T R A C T

In the present paper a new additive manufacturing processing route is introduced for ultra-high performance concrete. Interdisciplinary work involving materials science, computation, robotics, architecture and design resulted in the development of an innovative way of 3D printing cementitious materials. The 3D printing process involved is based on a FDM-like technique, in the sense that a material is deposited layer by layer through an extrusion printhead mounted on a 6-axis robotic arm. The mechanical properties of 3D printed materials are assessed. The proposed technology succeeds in solving many of the problems that can be found in the literature. Most notably, this process allows the production of 3D large-scale complex geometries, without the use of temporary supports, as opposed to 2.5D examples found in the literature for concrete 3D printing. Architectural cases of application are used as examples in order to demonstrate the potentialities of the technology. Two structural elements were produced and constitute some of the largest 3D printed concrete parts available until now. Multifunctionality was enabled for both structural elements by taking advantage of the complex geometry which can be achieved using our technology for large-scale additive manufacturing.

1. Introduction

Until recently, additive manufacturing (AM) techniques were confined to high value adding sectors such as the aeronautical and biomedical industries, mainly due to the steep cost of primary materials used for such processes. In the last decade, the development of large-scale AM in such domains as design, construction and architecture, using various materials such as polymers [19], metals [20] and cementitious materials [16]. The deposition process introduced in this paper is designed for cement-based 3D printing.

Historically, the first attempt at cement-based AM was made by [21] using an intermediate process between the classical powder bed and inkjet head 3D printing (3DP) [25] and fused deposition modeling (FDM) [8], in order to glue sand layers together with a Portland cement paste. Many groups have been involved with the development of large-scale AM for construction applications, all of which have been using processing routes derived from FDM or 3DP, although varying depending on the chosen material and targeted application.

Among the literature available, three projects stand out over the last decade.

- The pioneering Contour Crafting (CC) project [14] is based on the extrusion of two layers of cementitious materials in order to generate a formwork. The extruded piece surface roughness is smoothed out using a trowel while performing the extrusion. The 3D printhead is mounted on an overhead crane as the system is designed for on-site construction operations. There are several drawbacks with the technology developed by [14]: the CC technology is limited to vertical extrusion, hence yielding 2.5D topologies (vertical extension of a planar shape); the initial formwork and trowel system can be rather complex to implement for production, depending on the size and shape of the object being printed. Furthermore, the interrupted sequential casting of concrete within the formwork due to hydrostatic pressure and weak mechanical properties of the extruded cement ensure the occurence of weakened interfacial zones between the layers, as shown experimentally by [17].
- The on-going concrete printing project at Loughborough University [6] is to a certain extent similar to the CC project since the printhead used for deposition of cementitious materials is also mounted on an overhead crane [18]. The material used in this project is a high-performance concrete [17], yielding better material properties than was obtained in the CC project. The high mechanical performance of the material combined with the relatively small diameter of the extrudate (4 — 6 mm) [16] allow for a good geometrical control. However, the trade-off necessary for maintaining its dimensional accuracy

* Corresponding author at: PIMM, Arts et Métiers-ParisTech/CNAM/CNRS UMR 8006, 151 bd de l'Hôpital, 75013 Paris, France.
E-mail address: justin.dirrenberger@ensam.eu (J. Dirrenberger).

makes the process quite slow with regards to the envisioned industrial application. Although the project initially aimed at developing a processing system enabling for the generation of 3D topologies rather than 2.5D, the proposed solutions made use of supports, as in many other AM technologies, hence reducing the efficiency and flexibility of the process while increasing its material cost. Finally, dimensions and possibilities in terms of shape-design are prescribed by the use of an overhead crane.

- The D-Shape project [7], developed by Enrico Dini, is based on a 3DP-like technology. A large-scale sand-bed locally solidified by deposition of a binding agent, which is done using a printhead mounted on an overhead crane. This is done sequentially layer by layer; once the printing process is over, the printed piece is taken out of the sand bed; the remaining sand can be readily reused in the process. Although initially designed for the off-site production of panels as well as structural elements with complex geometries, the D-Shape project is currently aiming at demonstrating the feasibility of their process locally on-site, where only local construction material, i.e. sand, and binder materials can be used.

Based upon an understanding of the limitations identified in the above cited projects, the research project introduced in the present paper deals with the large-scale additive manufacturing of selective deposition for ultra-high performance concrete (UHPC). The 3D involved printing process is based on a FDM-like technique, in the sense that a material is deposited layer by layer through an extrusion printhead. The present work also explores the possibilities offered by computer-aided design (CAD) and optimization, and their integration within the product design process in the case of large-scale AM. Thus, the introduced technology succeeds in solving many of the problems that can be found in the literature. Most notably, the process introduced in the present paper enables the production of 3D large-scale complex geometries, without the use of temporary supports, as opposed to 2.5D examples found in the literature for concrete 3D printing. As a side remark, let us emphasize that the examples presented in this paper are among the largest 3D printed concrete parts ever produced. Multifunctionality enabled by arbitrary complex geometry is studied for a large-scale structural element. The research project presented in this paper was designed upon the following challenge: developing a large-scale additive manufacturing technology capable of producing multifunctional structural elements with increased performance. With this work, the aim of the authors is also to take part in the redefinition of architecture and design in the light of integral computation and fully automated processes.

The paper is organized as follows. First, the design and processing chain is described. The material considered for validating this new process route is presented and tested in Section 3. In Section 4 examples of complex shape structural elements produced with large-scale UHPC 3D printing are given. The obtained results are discussed in Section 5, as well as the techonolgy potential. Finally, in Section 6 a few concluding remarks are drawn.

2. Processing setup

2.1. Computational design

Generating and modeling shapes for additive manufacturing has to be done following specific sets of requirements, coming from both the processing constraints, e.g. layer thickness, product dimensions, etc., and the functional properties of the produced part, e.g. mechanical strength, thermal conductivity, etc. Both types of constraints will have to be considered synergetically at three different time and spatial scales: the material scale, the building path scale, and the global shape scale. In the present work, the processing constraints consist mainly in controling the rheology of the extruded paste and the setting kinetics of the material in interaction with the continuous building path and global shape of the object, e.g. a quickly setting mortar and/or a larger global shape allows for faster building path for a given layer. Functional requirements depend mostly on the properties of the hardened material and the structural geometry for effective mechanical properties, as well as other geometrically induced properties such as thermal insulation, soundproofing, etc.

Various approaches can be adopted for generating the robotic building path. An usual and straightforward method for generating a building path is to use a 3D-to-2D slicing software. It consists in slicing the 3D shape of an object in flat thin layers of constant thickness which can be layered one up onto the other. This results in a cantilever-method strategy, as shown on Fig. 1 (left). Each layer is then made of a contour line, as well as a filling pattern such as a honeycomb structure or a space-filling curve (Peano curve, Hilbert curve, etc.); the filling density can be adjusted for given requirements. This method is well-established for small-scale AM and 3D printing polymer- or metal-based processes. It is however not appropriate for large-scale AM since it does not take into account the processing constraints and their impact on the performance of the printed object. The building path should be adapted and optimized based on simulation results in order to take into account constraints and to exhibit more robustness for complex geometries.

These drawbacks are avoided in the present work by relying on a different method for generating a building path. The tangential continuity method (TCM) shown in Fig. 1 (right) is better for large-scale AM since the building paths are actually 3-dimensional, i.e. made of non-planar layers with locally varying thicknesses, hence better exploiting the geometrical potentialities of 3D printing technologies. The obvious advantage of such strategy is to keep contact surfaces constant between two layers, hence avoiding the geometrical gaps between two layers which often limit the possibilities of AM processes, most notably FDM and powder-bed-based processes. The layered structures obtained using the tangential continuity method can thus be mechanically loaded as classical masonry vaults, i.e. in pure compression, perpendicularly to the layer interface plane. Both methods are presented on Fig. 1: with the cantilever method the heigth of layers (grey) is preserved but the surface of contact varies (red), while the TCM preserves the surface of contact (red) and changes the height of layers (grey). From a structural mechanics viewpoint, the TCM yields more efficient and mechanically sound constructions.

2.2. Controlling the 6-axis robotic arm and printing system

For spatial displacement, an industrial ABB 6620 6-axis robotic arm was used. The remaining processing hardware parts were designed in-house. It consists in a printhead mounted on the robot as well as two peristaltic pumps, one for the premix and one for the accelerating

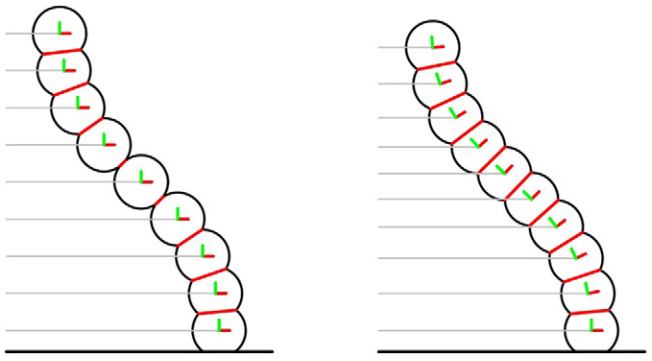

Fig. 1. Schematic cut perpendicular to layers 3D printed using the cantilever method commonly found in commercial 2D slicing software (left) and the tangential continuity method (right). (For interpretation of the references to color in this figure legend, the reader is referred to the web version of this article.)

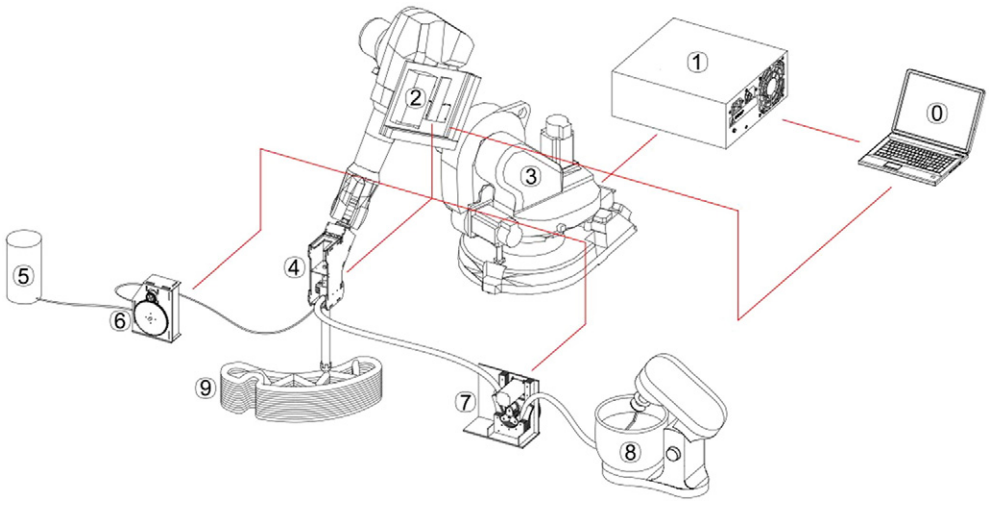

Fig. 2. Schematic of the 3D printing setup: 0. System command; 1. Robot controller; 2. Printing controller; 3. Robotic arm; 4. Printhead; 5. Accelerating agent; 6. Peristaltic pump for accelering agent; 7. Peristaltic pump for premix; 8. Premix mixer; 9. 3D printed object.

agent, and a premix mixer, all three parts deported from the robotic arm (see Fig. 2). Both pumps and the printead are controlled by an Arduino Mega 2560 micro-controller through a program controlling the printhead and pumps depending on the building path in order to deal with emergency stops and additives dosage.

From the software viewpoint, the 3D printing system if fully controlled via the Grasshopper/Rhino v.5.0 framework (McNeel, Seattle, WA). The HAL plug-in [26] was used to control the robotic arm, while the Firefly plug-in was used for interfacing the Arduino microcontroller with Grasshopper and controlling the printhead.

2.3. Printing process

The 3D printing process developed consists of two steps. First, a mortar premix prepared with a rheological behavior appropriate for pumping, i.e. with a fine particle-size distribution, low critical shear stress and slow hardening quality. The premix is kept in a shearing mixer in order to avoid setting due to its thixotropic behavior. The premix is then conveyed using a peristaltic pump towards a mixing screw located within the printhead. During this step, additives are dispersed in the mix in order to accelerate the setting of mechanical properties just after extrusion. The width of extrudate considered in this work is $w = 20$ mm.

3. Materials characterisation

A novel premix of cementitious material was used in this work. This material was specifically developed and supplied by LafargeHolcim for this project, with requirements regarding its workability in order to accelerate the printing process, and early age mechanical strength for layer-by-layer build-up capability. The premix is composed of original Portland cement CEM I 52.5N ($30-40\%_w$), crystalline silica ($40-50\%_w$), silica fume ($10\%_w$) and limestone filler ($10\%_w$). Once mixed with water in very small proportion (water/(cement + sand) mass ratio, i.e. $w/(c+s) = 0.1$), the material consists of an ultra-high perfomance self-placing mortar paste, with an added gripping polymer-based resin for enhancing the quality of interfaces between printed layers, and an accelerating and thresholding agent in order to obtain both the adequate rheology and a setting time compatible with 3D printing contingencies. It is worth noting that what is usually called ultra-high performance concrete (UHPC) in the literature and the industry, is not concrete per se, but rather a mortar paste with no coarse

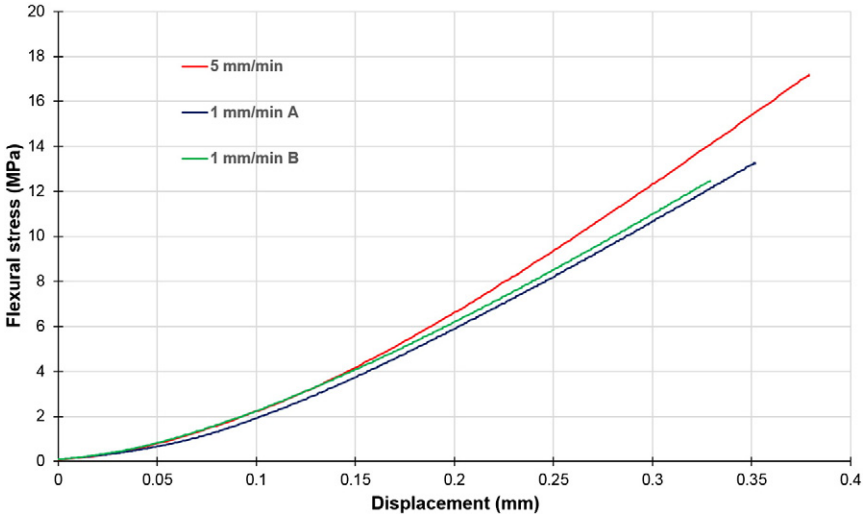

Fig. 3. Flexural stress vs. beam deflection for 4-point bending test on prismatic beams cut from 3D printed specimen.

aggregates (ø > 4 mm), which is the usual criterion for defining concrete. Nevertheless, the mechanical and thermal performance of UHPC, with or without reinforcements, is considerably superior to classical concrete. Mechanical characterisation was performed on 40×40×160 mm prismatic samples cut from 3D printed specimen which were cured at ambient temperature for 90 days. Flexural strength σ_f^* was estimated from 4-point bending tests according to ASTM C1161 experimental protocol, as the maximum value for flexural stress σ_f obtained following Eq. (1):

$$\sigma_f = \frac{3FL}{4b^3} \tag{1}$$

where F is the prescribed load and L the span between the supports, in the case of a square beam section of side b.

Samples were specifically cut in order to align perpendicularly the 3D printed layer interfaces to loading direction, i.e. along the length of the beam and horizontally with respect to the laboratory frame of reference. The span between the central supports was chosen to be 50 mm, while the distance between the first and last supports was 100 mm. The flexural stress vs. beam deflection results are presented in Fig. 3. Two strain rates (1 and 5 mm/min) were considered in order to exhibit the characteristic viscoelastic behavior of such cementitious materials. Three prismatic samples were tested for estimating the flexural strength. Failure of the mortar specimens took place within the pure bending zone of the samples, but no effect of layer interfaces was observed on the failure mechanisms.

The obtained value for flexural strength is $\sigma_f^* = 14.3 \pm 2.6$ MPa. The compressive strength σ_c^* can be estimated from the value of flexural strength and w/(c + s) mass ratio of the mortar. In this work, the ratio is very low ($w/(c+s) = 0.1$), given the specific nature of the material used. For such low $w/(c+s)$ ratios, the typical flexural to compressive strengths ratio is about 10% [22], hence yielding a conservative estimate for σ_c^* higher than 120 MPa, given a sound and homogeneous microstructure, which is similar although higher than what was obtained in the literature for a high-performance printing concrete [17]. This high mechanical performance allows for the fabrication of slender concrete-based structures, which is one of the main driving forces for considering large-scale 3D printing as an attractive alternative to more traditional methods such as casting.

4. Production of structural elements

As stated hereabove, the most attractive feature of 3D printing of concrete is the ability to produce complex 3D shapes in comparison to casting processes. In the field of architectural practice, a significant gap exists between the major part of nowadays architects seeking for lower cost, therefore resulting in simplistic and straight-shaped walls, while the remaining few ones who work on projects less constrained financially, can afford to design more complex forms, e.g. by designing customized molds and formworks for one-time use, thus generating large amounts of waste materials and unforeseen delays in the construction process. 3D printing is a disruptive technology which offers novel solutions that reconciliate non-standard shapes, and low costs. The structural parts developed in this work are loudspeaking examples of what can be achieved using this technology, hence pushing the boundaries of the design space available for engineers, architects and designers. Targeting unprecedented efficiency and/or multifunctionality through geometry can now be considered. Additional functions can be embedded in the structural parts, i.e. not only mechanical properties but also thermal insulation, soundproofing, etc. Two examples for large-scale application are presented in this paper, both consisting of structural wall elements. Both cases are relevant examples for demonstrating feasibility of the technology developed for application in architecture and construction.

4.1. Multifunctional wall element

This element was designed within a context of structural rehabilitation, starting from the damaged structure, i.e. one floor and its upper level without any structural support. The element was designed with the aim of optimizing what would become the external supporting wall, as shown on Fig. 4.

The element consists in an absorptive formwork to be filled either with ultra-high performance fibre-reinforced concrete on structural parts or with an insulating material such as foam for thermal insulation. Some parts are also left intentionally empty to be able to host pipes or electrical wires. The formwork has two column-like parts, linked to two straight plates in-between which waves a bi-sinusoidal shell.

Thermal insulation is an ever-increasing concern in construction; while the conductivity of concrete is usually of the order of $\lambda = 1 \mathrm{W.m^{-1}K^{-1}}$, the amount of heat flowing through the whole structural element can be reduced by optimizing the geometry. The thermal insulation efficiency of the wall lies in the reduction of thermal bridges. Because the total heat flux is proportional to the cross-section of the best conducting material in the system, i.e. concrete, the target for multiobjective optimization is to reduce the area of contact between two sides of the wall while maintaining its structural performance. Indeed, in the design considered, the only structural contacts are reduced to a few points, hence limiting the overall heat transfer between inner and outer faces. The shell considered is an egg-box, or 2D-sinusoidal, surface with angular frequency parameter ω such that its shape is described by Eq. (4):

$$z = \cos(\omega x)\cos(\omega y). \tag{2}$$

In order to formulate the thermal conduction problem, only a quarter of the 2D-sinusoidal period is considered due to symmetries. As a first-order approximation, this quarter of surface period is considered as planar for the sake of simplicity, with boundary conditions $T = 1$ for $z = 1$ and $T = -1$ for $z = -1$. Heat conservation is satisfied within this plane, as expressed in Eq. (3).

$$\nabla^2 T = 0 \tag{3}$$

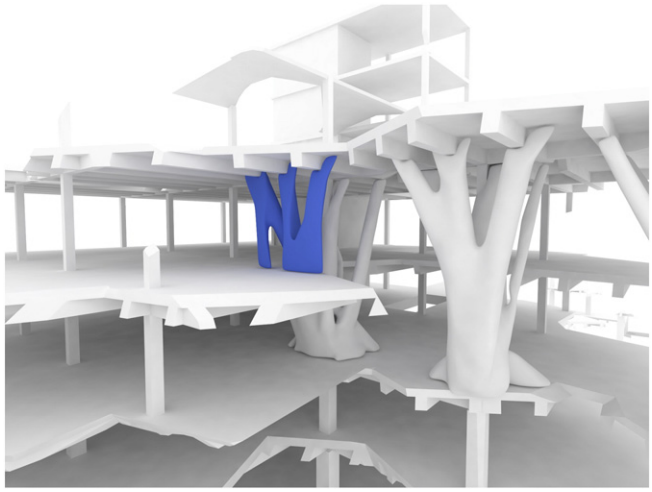

Fig. 4. Architectural context for the multifunctional wall element.

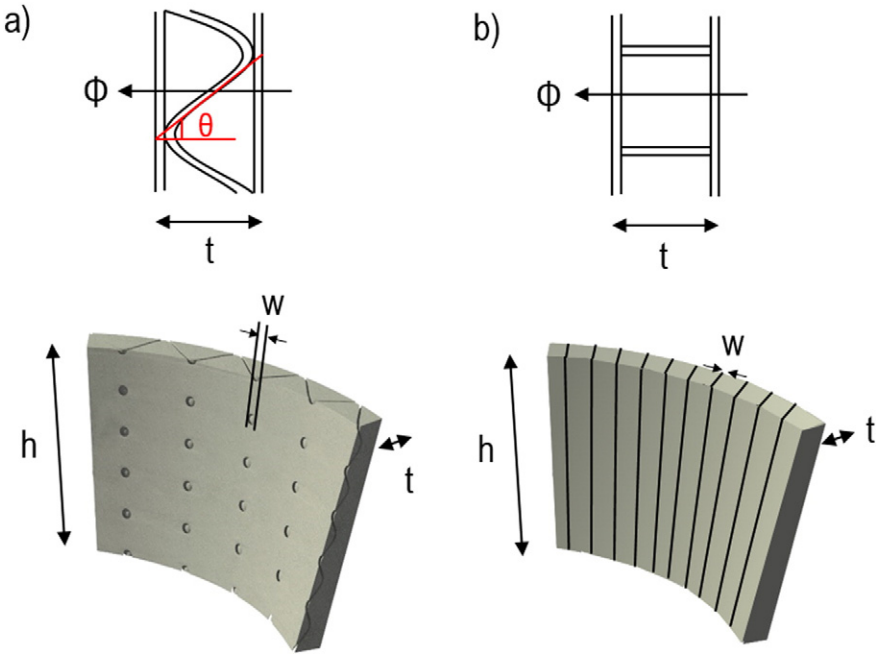

Fig. 5. Schematic description of 2 different designs for the multifunctional wall: 2-D sinusoidal shell reinforcement with ponctual contacts (a) or straight vertical reinforcement with linear contacts (b).

The total injected heat flux $\vec{\Phi}$ distributes equally in all directions within the plane, implying a heat flux density $\vec{\phi}$ written in Eq. (4) for polar coordinates (r,α) and shell thickness w:

$$\vec{\phi}(r,\alpha) = \frac{\vec{\Phi}}{2\pi r w}. \tag{4}$$

The radial component ∇T_r of the thermal gradient $\vec{\nabla} T$ can be written as Eq. (5) using Fourier's law, with $\vec{e}_r$ the radial unit vector:

$$\nabla T_r = -\frac{1}{\lambda}\vec{\phi}\cdot\vec{e}_r(r,\alpha) = -\vec{\Phi}\cdot\vec{e}_r\frac{1}{2\lambda\pi r w}. \tag{5}$$

The temperature field of obtained by integrating Eq. (5) with respect to r, as shown in Eq. (6) with the restriction that $r \neq 0$, corresponding to a singularity.

$$T = -\vec{\Phi}\cdot\vec{e}_r\frac{\ln r}{2\lambda\pi w} + cst \tag{6}$$

In order to avoid this situation, a non-zero radius of contact ρ is introduced, representing the contact area in a more realistic manner. The temperature field can thus be rewritten as Eq. (7) using the boundary value $T = 1$ for $r \leq \rho$.

$$T = 1 - \vec{\Phi}\cdot\vec{e}_r\frac{\ln\frac{r}{\rho}}{2\lambda\pi w} \tag{7}$$

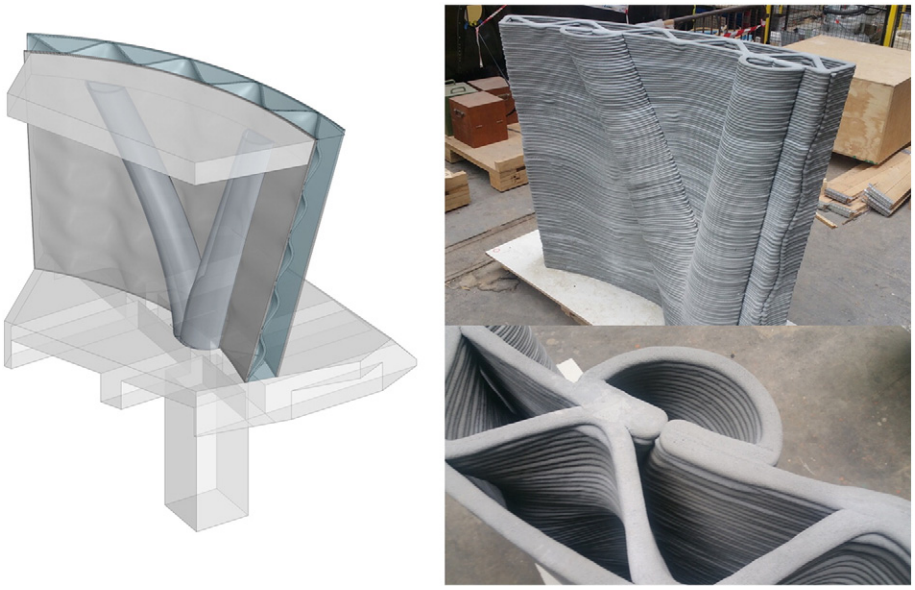

Fig. 6. CAD model for the multifunctionnal wall (left) and the 3D printed high-performance concrete multifunctionnal wall (right).

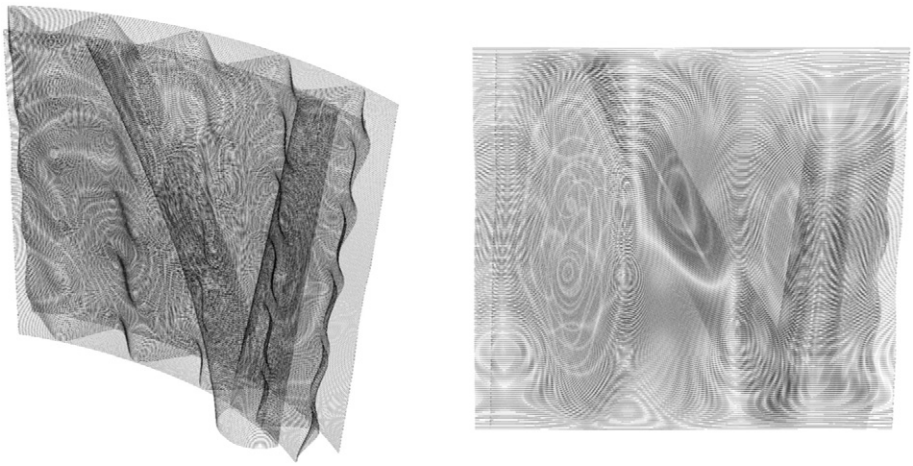

Fig. 7. Wireframe renderings of the continuous building path followed by the 6-axis robot while extruding UHPC for the multifunctionnal wall element.

For a distance $l/4$ corresponding to a quarter of the sinusoidal period, $T=0$ because of boundary conditions. Hence, using Eq. (7), the expression of total thermal heat flux $\vec{\Phi}$ can be deduced:

$$\vec{\Phi} = \frac{2\lambda\pi w}{\ln\frac{l}{4\rho}}\vec{e}_r. \tag{8}$$

The apparent thermal heat flux Φ^* through the wall thickness t over one period l is given by Eq. (9) for a temperature variation ΔT and apparent thermal conductivity K.

$$\Phi^* = \frac{\left\|\vec{\Phi}\right\|}{l^2} = \frac{\pi wt}{l^2\ln\frac{l}{4\rho}}\frac{\lambda\Delta T}{t} = K\frac{\Delta T}{t} \tag{9}$$

Hence, the ratio $a=K/k$ is an estimate of the thermal insulation performance for a given wall design, based on geometrical parameters only. From Fig. 5 can be deduced the ratio a for the two wall designs considered. For the first case (cf. Fig. 5a), $w=\rho=20$ mm, $t=170$ mm, $l=272$ mm, and $\theta\approx l/2t=53$ deg., which yields $a_1=11.8\%$. A second design with straight vertical reinforcements is shown in Fig. 5b. If one considers, for the sake of comparison, the thermal insulation performance at constant volume fraction of reinforcement, then $a_2=S/l^2=18.4\%$, which corresponds to the volume fraction of reinforcement within the wall, i.e. yielding an arithmetic average value for the apparent thermal conductivity.

The performance gain P in thermal insulation through geometric optimization for the multifunctional wall by comparison to a classical design, is obtained as follows:

$$P = \frac{a_2-a_1}{a_1} = 56\%. \tag{10}$$

Even by considering this simple first-order approximation, the reduction of thermal loss is tremendous, thus demonstrating the multifunctional character of the wall design proposed. A gain in thermal insulation performance of 56% was obtained in comparison to a classical wall design, only by optimizing the geometry of the internal reinforcement. Furthermore, the wavy shell is structurally efficient as it contains straight bars that form a stable truss, suited to support loadings. Also, the shell acts as a doubly-corrugated reinforcement, enhancing the flexural rigidity of the structure, similarly to cardboard. The production of the wall element took approximately 12 h (for 139 layers), its dimensions are roughly 1360 mm × 1500 mm × 170 mm, with a weight ca. 450 kg; the final wall is shown in Fig. 6. The continuous building path used for the production of this structural element is shown in Fig. 7. The resulting element could have hardly been produced using any other way, at least with any traditional or economically feasible processing route, hence emphasizing the interest of 3D printing in the field of construction. As a matter of fact, most of the production cost using the present technology is ascribable to workforce salary, which is typical of the construction industry. The CAD file representing this structural element is available with the online version of the present article as supplementary material, it could be used as a benchmark for large-scale 3D printing.

4.2. Acoustic damping wall element

Another example is the following element which was designed as a generic element both structural and acoustic performance, to be assembled alongside with others in order to form a complete wall. The different hole geometries could provide enhanced soundproofing properties to the element, by damping the acoustic waves passing through depending on the geometry of the wall cells and material properties. The produced element sizes roughly 650 mm × 650 mm × 300 mm and is shown in Fig. 8. It was printed in 2 h (26 layers), orthogonally to the plan of the wall in order to allow lace support.

Fig. 8. Concrete 3D printed acoustic damping wall element.

This is another example of what can be achieved using the technology presented in this paper, in terms of geometrical complexity and induced multifunctional properties.

5. Discussion

It was pointed out by [6] that the main interest for additive manufacturing applied to large scale construction would be neither speed nor cost, but rather an added value to the building element performance, mostly thanks to a clever use of geometry. Our work tries to address this geometrical challenge by understanding its crucial relation to material behavior and printing process. Although the early developments of large-scale cement-based AM processes have been linked to the concept of freeform, it appears rather difficult to separate each particular process from its reachable geometries. As a matter of fact, the Contour Crafting process [14], while being quite fast, is only limited to 2.5D extrusion shapes. The concrete printing process, mostly addressed by the team at Loughborough University [18], is conducted by a 3-axis deposition system that necessarily lacks precision when it comes to printing elements away from verticality. Our process achieves a new complexity for printable objects. The use of 6-axis industrial robot, enabled by the HAL Robotics software [26], not only allows non-horizontal and non-straight slicing of the printed object, but also eases the possibility of a true implementation of such technologies in the building industry, for it has not to be conducted with specifically developed machinery. The new printed material, developed with LafargeHolcim, brings an efficiency of fabrication speed and mechanical resistance never reached in the existing large-scale concrete-based AM projects. The fact that the material behavior at early and mature age influences the quality of the deposition process and the overall properties of the object, as well as the fact that the spatial disposition and morphology of interfaces between layers have an impact on the element behavior when loaded, make the term freeform unsuitable for describing such approaches. The design of the multi-purpose wall presented in this paper has not been conducted as a search for design freedom, but as an integrative approach, which makes clever use of geometry, understood as the result of a series of heterogeneous constraints. These constraints appear at each scale, from the complex structural build-up of the mortar to the need for adequate thermal properties of the full element. We believe we are at the beginning of a new understanding of geometrical design, enabled by such building processes, just as the iron and steel industry brought tremendous changes in construction during the second half of the XIXth century. The classical distinction between material and structure is fading quickly with AM techniques enabling the architecturation of materials at multiple scales, hence providing structural effects at the material level [2,4,5,15], as in the case of micro-architectured trusses [13], fractal trusses [23], hierarchical honeycomb structures [1], or auxetic materials [3,9–11]. From the viewpoint of construction and architecture, the distinction is also vanishing; there is a need for a new understanding of the concept of form, as an expression for the intersection of multiple flows of information [24] coming from the various aspects of the studied system. In such an interdisciplinary approach, the complexity and diversity of information is dealt with by making use of form-finding methods, meta-heuristic optimization algorithms and more conventional computational structural analysis techniques [12]. The design can be extracted from the heterogeneity of material, structural and architectural constraints, implemented in a computational modeling tool, which is fed and optimized accordingly by experimental feedback. The freedom of design will come from multidisciplinarity, by assessing every aspect of the engineering problem of interest, within a fruitful framework of interaction between computational modeling, experimental insight, and optimization.

6. Conclusions

Limitations of existing concrete-based AM projects have been reviewed and a novel process was proposed accordingly in this paper. The key characteristics of the present project can be summarized as follows:

- The possibility of producing large-scale 3D printed structures without temporary supports.
- The use of the tangential continuity method for slicing, hence fully exploiting the possibilities of 3D printing by creating layers with varying thickness, and resulting in, vault-like, mechanically sounder constructions from a structural viewpoint.
- Relying on a generic 6-axis robotic arm instead of an overhead crane, thus enabling geometrical complexity and total control through HAL [26].
- By enabling geometrical complexity, multifunctionality and structural effects can be induced in the printed objects, as showed by the examples of application presented.

Further work will include the use of multiple materials within the printing process in order to create gradients of material properties. The idea of using geometry for inducing functionality within structures will be studied further, as well as its relationship with the constructive process in architectural practice. Computational optimization tools will be adapted for multi-scale considerations, hence enabling the architecturation of matter from the microstructural scale up to the structural element scale.

Acknowledgements

This work is part of the DEMOCRITE (Large-scale additive manufacturing platform) Project. The authors would like to gratefully acknowledge *heSam Université* (grant PNM-14-SYNG-0002-01) for financial support through its *Paris Nouveaux Mondes* program.

References

[1] A. Adjari, B. Jahromi, J. Papadopoulos, H. Nayeb-Hashemi, A. Vaziri, Hierarchical honeycombs with tailorable properties, Int. J. Solids Struct. 49 (11 — 12) (2012) 1413–1419.
[2] M.F. Ashby, Y. Bréchet, Designing hybrid materials, Acta Mater. 51 (2003) 5801–5821.
[3] N. Auffray, J. Dirrenberger, G. Rosi, A complete description of bi-dimensional anisotropic strain-gradient elasticity, Int. J. Solids Struct. 69-70 (2015) 195–210.
[4] O. Bouaziz, Y. Bréchet, J.D. Embury, Heterogeneous and architectured materials: a possible strategy for design of structural materials, Adv. Eng. Mater. 10 (1–2) (2008) 24–36.
[5] Y. Bréchet, J.D. Embury, Architectured materials: expanding materials space, Scr. Mater. 68 (1) (2013) 1–3.
[6] R. Buswell, R. Soar, A. Gibb, A. Thorpe, Freeform construction: mega-scale rapid manufacturing for construction, Autom. Constr. 16 (2007) 224–231.
[7] G. Cesaretti, E. Dini, X.D. Kestelier, V. Colla, L. Pambaguian, Building components for an outpost on the lunar soil by means of a novel 3d printing technology, Acta Astronaut. 93 (2014) 430–450.
[8] S. Crump, Apparatus and Method for Creating Three-Dimensional Objects, 1992.
[9] J. Dirrenberger, S. Forest, D. Jeulin, Elastoplasticity of auxetic materials, Comput. Mater. Sci. 64 (2012) 57–61.
[10] J. Dirrenberger, S. Forest, D. Jeulin, Effective elastic properties of auxetic microstructures: anisotropy and structural applications, Int. J. Mech. Mater. Des. 9 (1) (2013) 21–33.
[11] J. Dirrenberger, S. Forest, D. Jeulin, C. Colin, Homogenization of periodic auxetic materials, Procedia Engineering, 10:1847–1852. 11th International Conference on the Mechanical Behavior of Materials (ICM11), 2011.
[12] R. Duballet, C. Gosselin, P. Roux, Additive Manufacturing and Multi-Objective Optimization of Graded Polystyrene Aggregate Concrete Structures, in: M. Thomsen, M. Tamke, C. Gengnagel, B. Faircloth, F. Scheurer (Eds.), Modelling Behaviour- Design Modelling Symposium 2015, Springer, 2016.
[13] N.A. Fleck, V.S. Deshpande, M.F. Ashby, Micro-architectured materials: past, present and future, Proc. R. Soc. A 466 (2121) (2010) 2495–2516.
[14] B. Khoshnevis, Automated construction by contour crafting- related robotics and information technologies, Autom. Constr. 13 (2004) 5–19.
[15] R.S. Lakes, Materials with structural hierarchy, Nature 361 (1993) 511–515.
[16] T. Le, S. Austin, S. Lim, R. Buswell, A. Gibb, T. Thorpe, Mix design and fresh properties for high-performance printing concrete, Mater. Struct. 45 (2012) 1221–1232.
[17] T. Le, S. Austin, S. Lim, R. Buswell, R. Law, A. Gibb, T. Thorpe, Hardened properties of high-performance printing concrete, Cem. Concr. Res. 42 (2012) 558–566.
[18] S. Lim, R. Buswell, T. Le, S. Austin, A. Gibb, T. Thorpe, Developments in construction-scale additive manufacturing processes, Autom. Constr. 21 (2012) 263–268.
[19] J. Menger, http://3dprint.com/52978/robotic-arm-3d-printer/2015.
[20] MX3D, http://mx3d.com/2015.

[21] J. Pegna, Exploratory investigation of solid freeform construction, Autom. Constr. 5 (1997) 427–437.
[22] S. Popovics, Strength and Related Properties of Concrete- A Quantitative Approach, Wiley, 1998.
[23] D. Rayneau-Kirkhope, Y. Mao, R. Farr, Ultralight fractal structures from hollow tubes, Phys. Rev. Lett. 109 (2012) 204301.
[24] D. Rebolj, M. Fischer, D. Endy, T. Moore, A. Sorgo, Can we grow buildings? Concepts and requirements for automated nano- to meter-scale building, Adv. Eng. Inform. 25 (2011) 390–398.
[25] E. Sachs, J. Haggerty, M. Cima, P. Williams, Three-Dimensional Printing Techniques, 1993.
[26] T. Schwartz, *HAL: Extension of a Visual Programming Language to Support Teaching and Research on Robotics Applied to Construction*, Springer, Vienna, 2012 92–101.